

Tribological properties of highly oriented Ti(C,N) deposited by chemical vapor deposition



L. von Fieandt^{a,*}, M. Fallqvist^b, T. Larsson^b, E. Lindahl^c, M. Boman^a

^a Uppsala University, Department of Chemistry – Ångström Laboratory, Lagerhyddsvägen 1, Box 538, 75120 Uppsala, Sweden

^b Seco Tools AB, Björnbacksvägen 2, 73782 Fagersta, Sweden

^c AB Sandvik Coromant, Lerkrogsvägen 19, 12679 Hägersten, Sweden

ARTICLE INFO

Keywords:

Hard coating
Coating adhesion
Abrasive wear
CVD coating

ABSTRACT

Two Ti(C,N) coatings were tested by means of micro abrasion and scratch testing. The coatings differed in grain size, orientation (<111> and <111>, <311> and <211> respectively) and hardness (36 GPa and 23 GPa respectively). The <111> oriented coating had a 20% higher wear resistance compared to the reference coating when abraded with 1 μm diamonds. When abraded with 6 μm diamonds the abrasion resistance of the reference coating was superior compared to the <111> oriented coating by 36%. Furthermore, it was found that the <111> oriented coating had 35% better adhesion compared to the reference. The improved mechanical properties of the <111> oriented coating was attributed to a high degree of orientation and the higher hardness.

1. Introduction

Surface modification by means of chemical vapor deposition (CVD) has been used to enhance material properties for decades. CVD is currently used in many different areas such as; electronics, photovoltaics, optics and protective coatings. Hard protective coatings by CVD are routinely used in the cutting tool manufacturing industry, where most of the tools have a multi-layer coating system, often in the sequence: TiN-Ti(C,N)-α-Al₂O₃. The TiN layer closest to the substrate serves to improve the adhesion between coating and substrate. The main function of the Ti(C,N) layer is to provide hardness and abrasion resistance. The, α-Al₂O₃, provides a combination of chemical inertness, good oxidation resistance and a high wear resistance.

Ti(C,N) is a solid solution of TiN and TiC, providing the benefits of both materials, i.e. chemical stability and inertness from TiN and a high hardness from TiC [1]. It has been shown that the carbon to nitrogen ratio in Ti(C,N) has a great impact on the hardness of the material, where a carbon rich Ti(C,N) is harder [2–5]. The grain size is another aspect that affects the hardness. It is well known that a more fine grained coating will increase the hardness. Additionally, it has been shown that the hardness of a cubic material is dependent on the crystallographic orientation of the material and is therefore not isotropic. It was shown that a <111> oriented TiC single crystal showed a more homogeneous hardness than single crystals of other orientations [6,7]. This suggests that a <111> oriented coating may have improved mechanical properties compared to

other orientations. It has been shown that by tuning the crystallographic orientation and morphology of CVD deposited Ti(C,N) from a <211> texture with fine grains to a <111> texture with large (>3 μm sized) grains, the coating hardness could be increased significantly [8].

One of the main wear mechanisms for a cutting tool is abrasive wear, where hard inclusions in the work piece material act as abrasive particles on the tool [9]. The abrasion resistance is greatly improved by applying a coating having a higher hardness than the compound hardness of the cemented carbide substrate [10]. It is therefore not surprising that by optimizing the coating orientation with respect to hardness will increase the resistance to abrasive wear [11,12].

Apart from the wear resistance of the coating, the lifetime of a cutting tool is strongly dependent on the adhesion between the tool and the coating, where a poor adhesion is detrimental for tool life. Scratch testing is a commonly used technique for testing adhesion of hard coatings. In previous studies it was shown that several aspects influenced the tool-coating adhesion i.e. coating thickness, substrate hardness, coating hardness and coating – indenter friction coefficient etc. [13–15].

The mechanical properties, such as hardness, adhesion and sliding wear resistance, of Ti(C,N) coatings grown by different techniques have been studied [16]. Commercially available CVD Ti(C,N) showed a similar wear resistance as Ti(C,N) layers deposited by PVD techniques, despite having a lower hardness [16]. This shows that the hardness of the coating is not the only factor influencing the wear resistance. The microstructure, orientation, grain size and surface morphology of the coatings will also

* Corresponding author.

E-mail address: linus.fieandt@kemi.uu.se (L. von Fieandt).

affect the wear resistance [17,18].

CVD Ti(C,N) deposited at conditions described in Refs. [16,19] are typically <211> orientated and have a ridge like grain morphology [2–4,20,21]. The resistance to flank and abrasive wear of <211> oriented Ti(C,N) were improved by reducing the grain size, increasing the carbon content and a higher degree of <211> orientation [4]. There is no study available where CVD-Ti(C,N) coatings of different orientations having the same composition are compared. In this investigation the mechanical properties of highly <111> oriented Ti(C,N) with large grains was compared to a fine-grained Ti(C,N) reference coating with multiple orientations, i.e. <111>, <311>, <211> and <511>.

2. Material and methods

2.1. Materials

Two Ti(C,N) coatings of the same composition, $Ti(C_{0.6},N_{0.4})_{0.8}$ but with different crystallographic orientation were deposited by CVD to a thickness of about 6 μm , for deposition conditions see Table 1. The coating, hence forth known as the <111> oriented coating, had a hardness of 36 GPa and was entirely <111> orientated with large grains (>3 μm). The reference coating, had several orientations (<111>, <311> and <211>) and a smaller grain size (<0.5 μm). The hardness of the reference coating was 23 GPa. The hardness of both coatings was measured by nanoindentation. The stress states were similar to those found in a previous report of similar coatings [8]. The Ti(C,N) coatings investigated in the present study were deposited using a Bernex 530 hot-wall CVD reactor. $10 \times 10 \times 0.5$ mm polished single crystal c-sapphire supplied from MTI Corp was used as substrates.

2.2. Characterization methods

2.2.1. Rocking curve measurements (ω -scans)

Rocking curve measurements were conducted in order to determine the degree of orientation for each coating. A Philips MRD X-pert diffractometer equipped with a primary hybrid monochromator and diffracted beam mirror, Cu-K α radiation was used in the measurements.

2.2.2. Micro abrasion

Micro abrasion tests were performed using a Gatan 656 dimple grinder equipped with a stainless steel wheel ($r = 10$ mm) applying a constant load of 0.2 N and a rotation speed of 100 rpm. A diamond slurry of 1 and 6 μm diamond particles respectively (Kemet[®] Liquid diamond Type WX XStr) were used. In order to keep the resulting craters within the thickness of the coatings, the grinding time was set to 5 s. Five craters for each particle size were made on each coating. The diameter of the craters was measured using an optical microscope. The global wear volume (V_g) and the wear rate (κ) was calculated using the following equations [22,23]:

$$V_g \approx \frac{\pi b^4}{64R} \quad (\text{for } b < R) \quad (1)$$

$$SL = \frac{V_g}{\kappa} \quad (2)$$

Where b is the outer diameter of the crater, R is the radius of the wheel, S is the sliding distance of the wheel and L is the normal load.

Table 1

Deposition parameters for both coatings, deposition time, total pressure and temperature was 5 h, 8 kPa and 860 °C respectively for both coatings.

Coating	H ₂ partial pressure (kPa)	N ₂ partial pressure (kPa)	TiCl ₄ partial pressure (kPa)	CH ₃ CN partial pressure (kPa)	Total flow (l/min)
<111> oriented	Balance	0.98	0.11	0.05	82
Reference	Balance	0.98	0.19	0.05	82

2.3. Scratch testing

The cohesive strength and adhesion of the coatings were investigated using a Micro scratch tester (Anton Paar Revetest) equipped with a 200 μm Rockwell C diamond stylus and applying an increasing load from 1 to 50 N over a scratch length of 3 mm with a linear load increase.

Further scratch testing were performed using a 10 μm Rockwell C diamond stylus. For the 10 μm stylus the load was varied between 1 and 5 N and the scratch length was 3 mm applying a linear load increase.

2.4. Microstructure and surface analysis

The microstructure and surface morphology of the tested coatings were analyzed using a Zeiss-Merlin high resolution scanning electron microscope (SEM) operating at a 3 kV accelerating voltage. Optical images were acquired using a Alicona infinite focus microscope. The R_a surface roughness of the coatings was measured using a WYKO NT1100 optical profilometer.

3. Results

3.1. As-deposited material

The surface morphology of the investigated coatings is shown in Fig. 1. Where the <111> oriented coating has large and flat grains (Fig. 1a) and the reference coating with several crystallographic orientations have small ridge like grains (Fig. 1b). The R_a surface roughness was 140 nm for the <111> oriented coating and 20 nm for the reference coating.

The degree of orientation of the coatings was evaluated by ω -scans, see Fig. 2. The <111> oriented coating had a ω full width at half maximum (FWHM) measured on the (111) peak of 0.3°, see Fig. 2a. No ω peaks were observed for any of the other planes, showing that the coating was entirely <111> orientated. The reference coating had several crystallographic orientations. The strongest peaks came from the (111), (311) and (422) planes with a FWHM of 1.4, 5.0 and 4.2°, respectively, see Fig. 2b–d. This shows that the <111> oriented coating is singly oriented with a small FWHM while the reference coating show multiple orientations where each orientation has a larger FWHM compared to the <111> oriented coating.

3.2. Micro abrasion

Analysis of crater volumes and wear rates by optical microscope are presented in Fig. 3. The <111> oriented coating had a **20% smaller** crater volume compared to the reference coating when using 1 μm particles. The crater volume was **36% larger** for the <111> oriented coating when using 6 μm particles. The micro abrasion is showing a lower wear rate for the <111> oriented coating for the test with 1 μm diamond particles compared to the reference. The relationship is the opposite when using 6 μm diamond particles, where the <111> oriented coating had a higher wear rate than the reference coating.

Figs. 4 and 5 show analysis of the crater center after initial contact. Micro cutting and micro chipping were identified as the dominating abrasive wear mechanisms. Micro cutting is a result of diamond particle cutting the coating, whereas microchipping is a result of cohesive failure in micro scale within the coating. The abrasion using 1 μm diamonds is shown in Fig. 4. The <111> oriented coating show a surface where minor

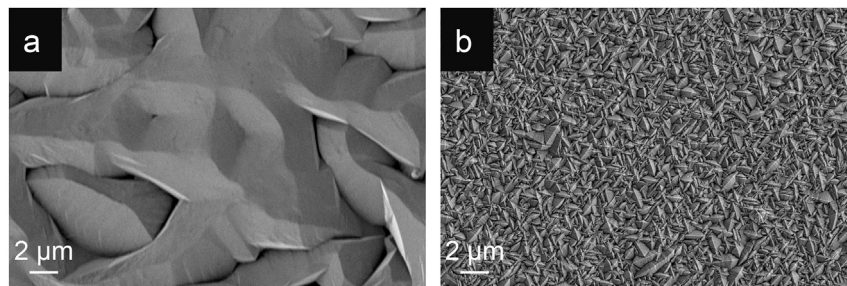


Fig. 1. SEM top view micrographs of the as-deposited coatings: a) <111> oriented coating, b) reference coating.

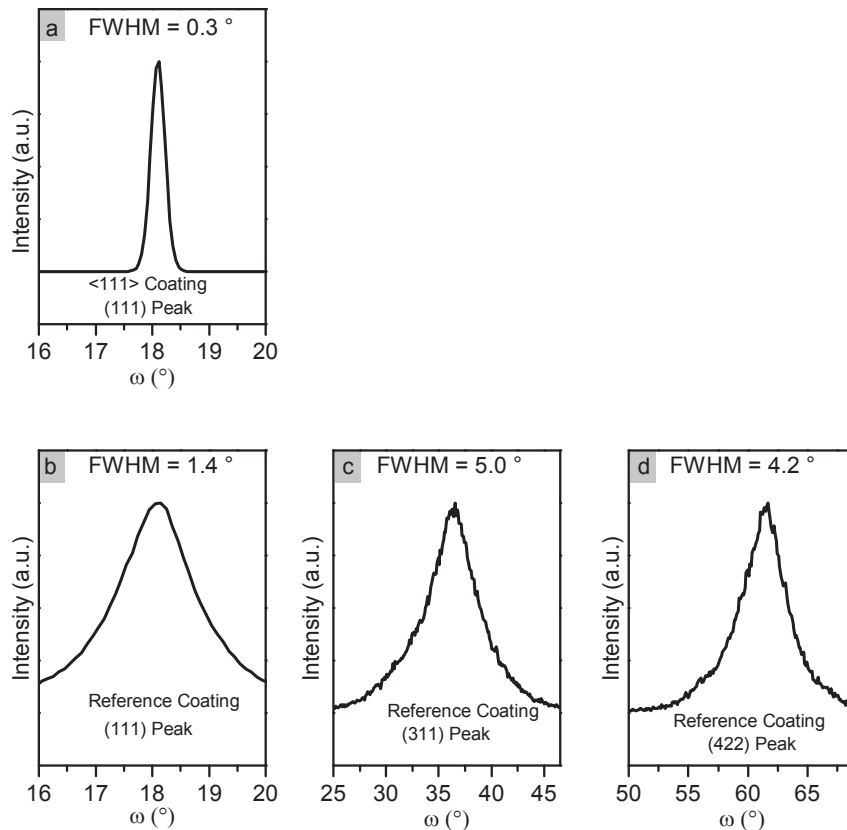


Fig. 2. ω -scan FWHM of: a) <111> oriented coating (111) peak, b) Reference coating (111) peak, c) Reference coating (311) peak, d) Reference coating (422) peak.

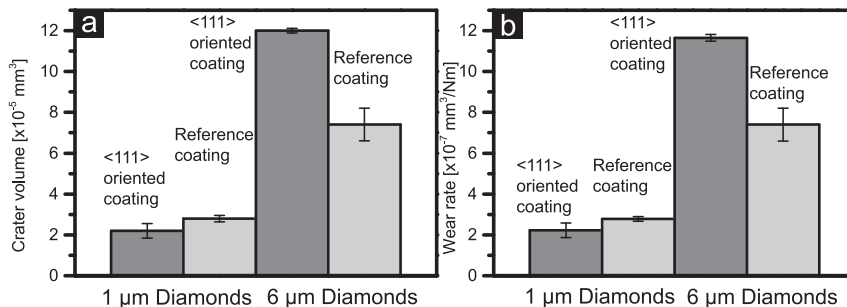


Fig. 3. Summary of results from micro abrasion tests for the coatings: a) wear crater volume b) abrasive wear rate.

micro cutting as well as micro chipping has been the main wear mechanisms, see Fig. 4a. It should be noted that parts of the pristine surface topography for the <111> oriented coating is still visible after initial wear. On the contrary, the pristine surface topography of the reference

coating is completely obliterated, see Fig. 4b. As such, the reference coating shows a more pronounced micro cutting with larger scratches and micro chipping to a small extent.

Abrasion using larger particles increases the deformation depth and

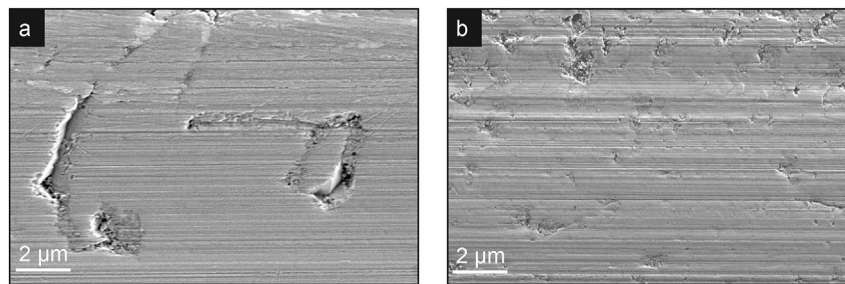


Fig. 4. SEM micrograph from the center of the craters for the coatings after initial contact (1 s) using 1 μm diamonds: a) <111> oriented coating b) reference coating.

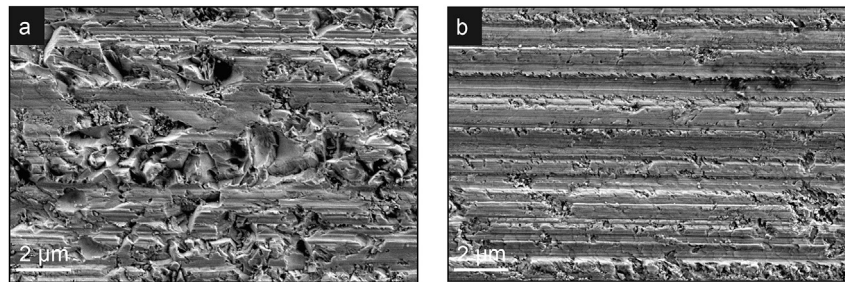


Fig. 5. SEM micrograph from the center of the craters for coatings after initial contact (1 s using 6 μm diamonds: a) <111> oriented coating b) reference coating.

gives a more aggressive contact. As a result the <111> oriented coating show an extensive wear from micro chipping when abraded with 6 μm diamond particles, see Fig. 5a, whereas the micro cutting still is limited. The reference coating exhibit a higher degree of plastic deformation (ploughing) with extensive micro cutting and mild micro chipping, see Fig. 5b.

In summary, the micro abrasion tests show that the <111> oriented coating has a higher resistance to abrasive wear when 1 μm diamond particles are used. However, when 6 μm diamond particles are used the reference coating performs better.

3.3. Scratch testing

3.3.1. 200 μm stylus

Two critical loads were determined for each coating: L_{c1} , corresponds to the onset of crack formation and L_{c2} , corresponding to the onset of continuous coating spalling. L_{c1} was determined through acoustic emission (AE) in the scratch tester and L_{c2} was determined by measurements in the SEM.

The AE signal from scratch testing for the <111> oriented coating is shown in Fig. 6a, where it can be seen that the L_{c1} for this coating is $10 \text{ N} \pm 0.6 \text{ N}$. This force corresponds to a sliding distance of roughly 0.6 mm. An optical overview image of the wear track is shown in Fig. 6b where the zones for L_{c1} and L_{c2} are marked. At L_{c1} , shown in Fig. 6c the grains were not deformed, although cracks were formed. At L_{c2} , which occurs at $37 \text{ N} \pm 1.4 \text{ N}$ according to Fig. 6d, the coating has spalled off the substrate and severe deformation can be seen in the wear track. Cracks are extending outside the wear track. The average friction between the stylus and the coating surface was determined to 0.11. The friction was determined in the area where no significant changes in AE occurred, i.e. 0–0.2 mm sliding distance.

For the reference coating with multiple orientations L_{c1} was determined to $8 \text{ N} \pm 0.5 \text{ N}$, see Fig. 7a by AE, corresponding to a sliding distance of 0.5 mm. An optical overview image of the scratch is presented in Fig. 7b where two areas are marked, corresponding to L_{c1} and L_{c2} . At L_{c1} , see Fig. 7c the coating is heavily plastically deformed in the wear track and cracks appear both inside and outside the wear track. At L_{c2} , see Fig. 7d, the coating has spalled from the substrate and cracks are

extending out from the wear track. L_{c2} occurred at $27.5 \text{ N} \pm 0.33 \text{ N}$, corresponding to a sliding distance of 1.6 mm. The average friction between the stylus and the coating surface was determined to 0.12. The friction was determined during the first 0.2 mm where no changes in the AE occurred.

3.3.2. 10 μm stylus

Scratch testing using a 10 μm stylus gives a more superficial contact but also a higher deformation rate than a 200 μm stylus does. Hence the cohesive strength of the coating is measured to a greater extent. The results from the scratch tests using the 10 μm stylus are presented in Fig. 8. The <111> oriented coating exhibited delamination after roughly 1.4 mm, corresponding to a normal load of 2.3 N, see Fig. 8a. This is significantly higher than the reference coating which delaminates after roughly 1 mm, corresponding to a normal load of 1.7 N, see Fig. 8b. Fig. 8a and b shows that the reference coating had a much more severe cracking behavior outside the wear track indicating a lower cohesive strength of this coating.

4. Discussion

The two investigated CVD-Ti(C,N) coatings differed significantly in their tribological properties. In this investigation the <111> oriented coating showed superior properties in the scratch test and the abrasion test when using 1 μm diamonds.

The better abrasion resistance for the <111> oriented coating using 1 μm diamonds can be attributed to the higher hardness of this coating compared to the reference coating, leading to a lower degree of micro cutting which is the dominating wear mechanism. The reversed relationship for the abrasion using 6 μm diamonds is most likely caused by the extensive micro chipping for the <111> oriented coating. This can be explained by considering the relationship between the coating grain size and abrasive particle size. The reference coating has a grain size around 500 nm, i.e. significantly smaller than both abrasive particle sizes, thus similar wear mechanisms were observed in both tests. On the contrary, the <111> oriented coating had a grain size of several microns, which means that a change from 1 μm to 6 μm particles to a large extent change the relationship particle-coating grain size. Small particles cut the surface

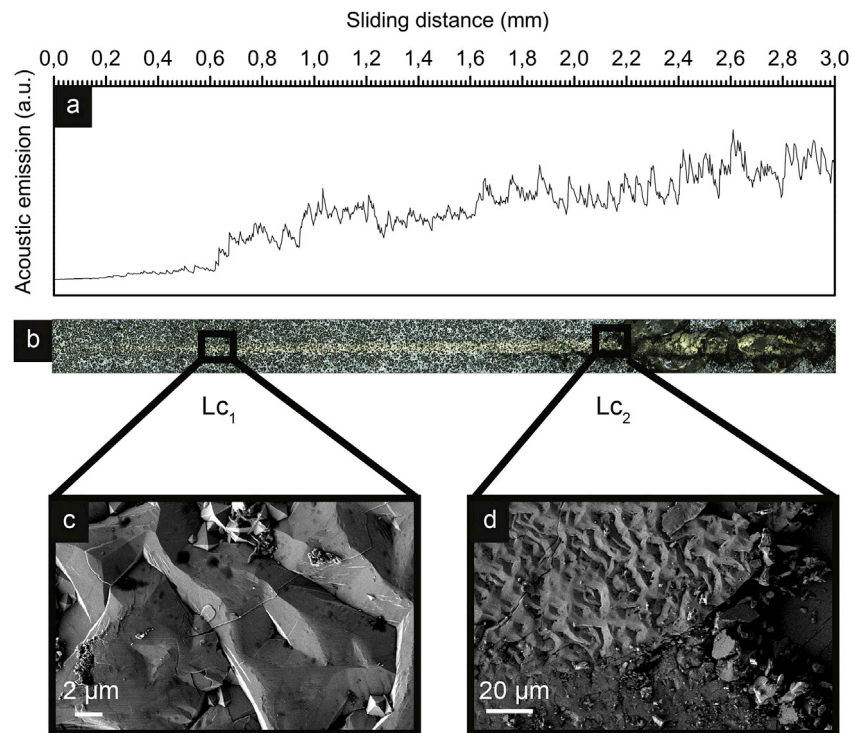


Fig. 6. Scratch test of the $\langle 111 \rangle$ oriented coating: a) representative AE signal, b) optical micrograph overview of the 3 mm wear track positions for Lc_1 and Lc_2 marked in the image, c) SEM micrograph of the wear at Lc_1 , d) SEM micrograph of the wear at Lc_2 .

in a smooth manner but the larger particles having about the same size as the coating grains will cause a pronounced micro chipping where entire grains from the coating are removed. Furthermore, the rougher surface of the $\langle 111 \rangle$ oriented coating (140 nm) compared to the reference coating (20 nm) could further explain the difference in micro chipping. Diamond

particles are more likely to be stuck in between the large grains of the $\langle 111 \rangle$ oriented coating and thereby will a high shear stress be generated locally. Micro chipping is a more aggressive type of wear than micro cutting, resulting in an increased wear rate for the $\langle 111 \rangle$ oriented coating in the test using 6 μm diamonds.

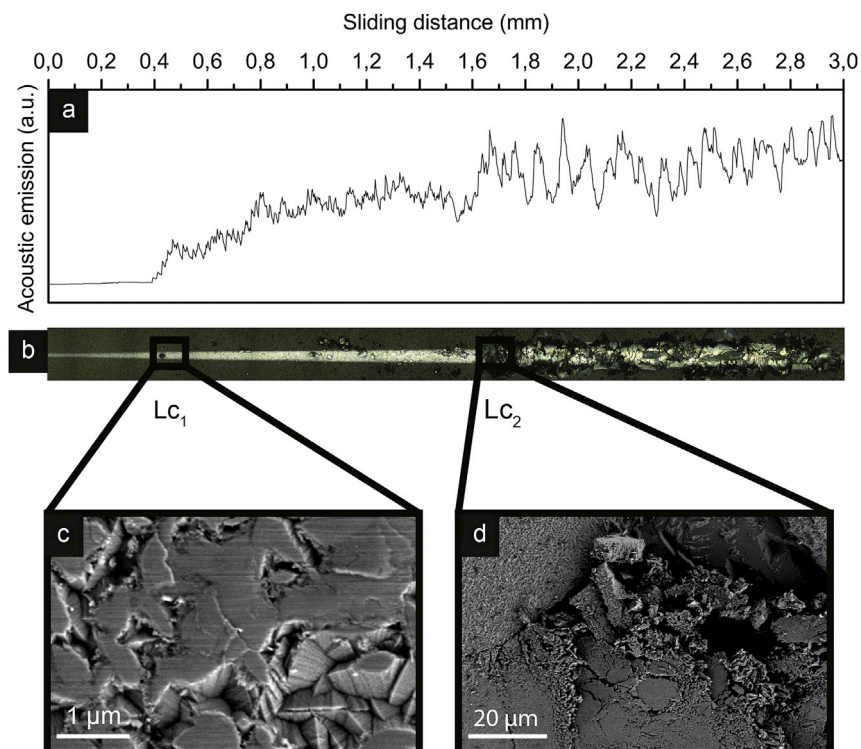


Fig. 7. Scratch test of the reference coating: a) representative AE signal, b) optical micrograph overview of the 3 mm wear track positions for Lc_1 and Lc_2 marked in the image, c) SEM micrograph of the wear at Lc_1 , d) SEM micrograph of the wear at Lc_2 .

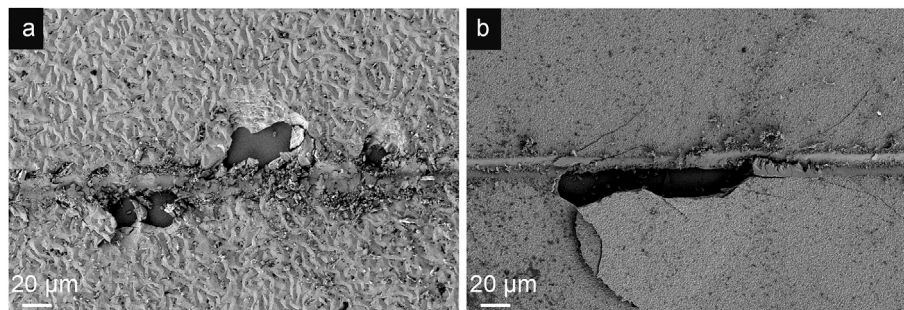


Fig. 8. Scratch tests using 10 µm stylus. Images taken at first continuous spalling: a) <111> oriented coating after 1.4 mm sliding, b) reference coating after 1 mm sliding.

The origin of the cracking behavior of the <111> oriented coating is somewhat counter intuitive, as harder ceramic materials normally exhibit cracking to a greater extent than softer equivalents [24]. The greater load bearing characteristics of the harder coating lowered the penetration depth of the diamond stylus. This prevented the diamond stylus from penetrating deep in to the coating. Therefore, the onset of crack formation started at a higher load than for the softer reference coating. This can partially explain the improved crack resistance. The reference coating changed the crystallographic orientation during growth. During initial growth it had a <111> orientation but switched to <311>/<211> at a later stage, thereby creating an orientation interface in the coating [8,25,26]. This interface can act as a mechanically weak area within the coating and lower the onset for crack formation and coating spalling. It should also be noted that the <111> oriented coating not only had a better cohesive strength but also better adhesion to the substrate.

A coating with a higher degree of orientation (small ω) has a lower degree of misorientation across grain boundaries, thus making the grain boundaries stronger. A low degree of misorientation between two grains will make it easier to deform the material over the grain boundaries without formation of cracks, thereby increasing the cohesive strength and making such a coating less prone to crack. Furthermore, the observed difference in surface roughness is not likely to affect the results in the scratch test as the radii of both indenters are orders of magnitude larger than the roughness. This is demonstrated by the small difference in friction coefficient between the coatings during the scratch testing (0.11 and 0.12 for <111> oriented and reference respectively). Assuming that the tip radii of the diamond particles used in the micro abrasion is significantly smaller than that of the indenters used in the scratch testing the micro abrasion tests are more likely to be affected by the surface roughness. This can explain the difference in chipping behavior between the abrasion testing and the scratch testing where the scratch indenters deform several grains at a time and thereby benefiting to a greater extent from the higher degree of orientation compared to the diamond particles in the abrasion tests.

In previous studies, a state of compressive stress has been shown to increase the hardness and crack resistance of a coating [27,28]. However, the stress states measured in a previous study indicates that the difference between the coatings is most likely too small to be the sole contributor to the differences in mechanical properties [8]. In summary, present results show that the <111> oriented coating has a combination of high resistance to abrasive wear, high coating cohesion and good adhesion. However, in contacts where micro chipping is the dominating wear mechanism the <111> oriented coating was worn out rapidly.

5. Conclusions

In this study two 6 µm thick $\text{Ti}(\text{C}_{0.6}\text{N}_{0.4})_{0.8}$ coatings of different orientation, microstructure and hardness were tested with respect to abrasion resistance, crack resistance/coating cohesion and adhesion. The tribological properties were evaluated by abrasion using 6 and 1 µm

diamond slurries and scratch testing using 200 µm and 10 µm Rockwell indenters.

It was found that the <111> oriented coating exhibited a 20% better resistance to abrasive wear compared to the reference coating with multiple orientations when abraded using 1 µm diamonds. For the abrasion using 6 µm diamonds the reference coating had a 36% better resistance to abrasive wear, due to extensive micro chipping of the <111> oriented coating. Furthermore, the <111> oriented coating exhibited superior resistance to crack formation (25%) and improved adhesion (35%) compared to the reference coating. Hence, the <111> oriented coating shows a noteworthy combination of both high hardness and high toughness.

The superior mechanical properties of the <111> oriented coating were attributed to the higher degree of orientation and higher hardness compared to the reference coating. It follows that with a higher degree of orientation comes a higher grain boundary cohesion that improves the grain boundary strength, which further serves to improve the mechanical properties.

Acknowledgements

Funding of CVD 2.0 by the Swedish Foundation for Strategic Research via SSF contract RMA15-0048 is gratefully acknowledged. Funding from Sandvik AB is gratefully acknowledged.

References

- [1] Odell F. Phase relationships in the binary systems of nitrides and carbides of zirconium, columbium, titanium, and vanadium. *J Electrochem Soc* 1950;97:299–304.
- [2] Garcia J, Pitonak R, Weissenbacher R, Köpf A. Production and characterization of wear resistant Ti(C,N) coatings manufactured by modified chemical vapor deposition process. *Surf Coatings Technol* 2010;205:2322–7. <https://doi.org/10.1016/j.surfcoat.2010.09.013>.
- [3] Paseuth A, Fukui H, Okuno S, Kanaoka H, Okada Y. Microstructure, mechanical properties, and cutting performance of TiC_xN_{1-x} coatings with various x values fabricated by moderate temperature chemical vapor deposition. *Surf Coatings Technol* 2014;260:139–47. <https://doi.org/10.1016/j.surfcoat.2014.09.068>.
- [4] Paseuth A, Fukui H, Yamagata K. Surface & Coatings Technology Improvement of mechanical properties and cutting performance of modified MT-TiC_xN_{1-x} coating by moderate temperature chemical vapor deposition. *Surf Coat Technol* 2016;291:54–61. <https://doi.org/10.1016/j.surfcoat.2016.02.023>.
- [5] Yasuoka M, Wang P, Murakami Richi. Comparison of the mechanical performance of cutting tools coated by either a TiC_xN_{1-x} single-layer or a TiC/TiC_{0.5}N_{0.5}/TiN multilayer using the hollow cathode discharge ion plating method. *Surf Coatings Technol* 2012;206:2168–72. <https://doi.org/10.1016/j.surfcoat.2011.09.053>.
- [6] Hannink RHJ, Kohlstedt DL, Murray MJ. Slip system determination in cubic carbides by hardness anisotropy. *Proc R Soc A* 1972;326.
- [7] Kumashiro Y, Itoh A, Kinoshita T, Sobajima M. The micro-Vickers hardness of TiC single crystals up to 1500 °C. *J Mater Sci* 1977;12:595–601. <https://doi.org/10.1007/BF00540285>.
- [8] von Fieandt L, Johansson K, Larsson T, Boman M, Lindahl E. On the growth, orientation and hardness of chemical vapor deposited Ti(C,N). *Thin Solid Films* 2018;645:19–26. <https://doi.org/10.1016/j.tsf.2017.10.037>.
- [9] Bejjani R, Collin M, Thersleff T, Odelros S. Multi-scale study of initial tool wear on textured alumina coating, and the effect of inclusions in low-alloyed steel. *Tribol Int* 2016;100:204–12. <https://doi.org/10.1016/j.triboint.2016.01.021>.

- [10] Duszová A, Halgaš R, Bl'anda M, Hvidzdoš P, František L, Dusza J, et al. Nanoindentation of WC – Co hardmetals. *J Eur Ceram Soc* 2013;33:2227–32. <https://doi.org/10.1016/j.jeurceramsoc.2012.12.018>.
- [11] Fallqvist M, Olsson M, Rупpi S. Abrasive wear of texture-controlled CVD α -Al₂O₃ coatings 2007;202:837–43. <https://doi.org/10.1016/j.surfcoat.2007.06.063>.
- [12] Batista JCA, Joseph MC, Godoy C, Matthews A. Micro-abrasion wear testing of PVD TiN coatings on untreated and plasma nitrided AISI H13 steel. *Wear* 2001;249: 971–9. [https://doi.org/10.1016/S0043-1648\(01\)00833-X](https://doi.org/10.1016/S0043-1648(01)00833-X).
- [13] Burnett PJ, Rickerby DS. The relationship between hardness and scratch adhesion. *Thin Solid Films* 1987;154:403–16.
- [14] Jindal PC, Quinto DT, Wolfe GJ. Adhesion Measurement of chemically vapor deposited and physically vapor deposited hard coatings on WC-Co substrates. *Thin Solid Films* 1987;154:361–75.
- [15] Perry AJ. Scratch adhesion testing of hard coatings. *Thin Solid Films* 1983;107: 167–80.
- [16] Bull SJ, Bhat DG, Staia MH. Properties and performance of commercial TiCN coatings. Part 2: tribological performance. *Surf Coatings Technol* 2003;163–164: 507–14. [https://doi.org/10.1016/S0257-8972\(02\)00651-5](https://doi.org/10.1016/S0257-8972(02)00651-5).
- [17] M'Saoubi R, Alm O, Andersson JM, Engström H, Larsson T, Johansson-Jöesaar MP, et al. Microstructure and wear mechanisms of texture-controlled CVD α -Al₂O₃ coatings. *Wear* 2017;376–377:1766–78. <https://doi.org/10.1016/j.wear.2017.01.071>.
- [18] Kumar DD, Kumar N, Kalaiselvam S, Radhika R, Maximus Rabel A, Jayavel R. Tribo-mechanical properties of reactive magnetron sputtered transition metal carbide coatings. *Tribol Int* 2017;114:234–44. <https://doi.org/10.1016/j.triboint.2017.04.031>.
- [19] Bull SJ, Bhat DG, Staia MH. Properties and performance of commercial TiCN coatings. Part 1: coating architecture and hardness modelling. *Surf Coatings Technol* 2003;163–164:499–506. [https://doi.org/10.1016/S0257-8972\(02\)00650-3](https://doi.org/10.1016/S0257-8972(02)00650-3).
- [20] Holzschuh H. Chemical-vapor deposition of wear resistant hard coatings in the Ti-B-C-N system: properties and metal-cutting tests. *Int J Refract Met Hard Mater* 2002; 20:143–9. [https://doi.org/10.1016/S0263-4368\(02\)00013-6](https://doi.org/10.1016/S0263-4368(02)00013-6).
- [21] Larsson A, Rупpi S. Microstructure and properties of Ti(C,N) coatings produced by moderate temperature chemical vapour deposition. *Thin Solid Films* 2002;402: 203–10. [https://doi.org/10.1016/S0040-6090\(01\)01712-6](https://doi.org/10.1016/S0040-6090(01)01712-6).
- [22] Çalıřkan H. Effect of test parameters on the micro-abrasion behavior of PVD CrN coatings. *Measurement* 2014;55:444–51. <https://doi.org/10.1016/j.measurement.2014.05.036>.
- [23] Parreiras Marques F, César Bozzi A, Scandian C, Paulo Tschiptschin A. Microabrasion of three experimental cobalt-chromium alloys: wear rates and wear mechanisms. *Wear* 2017;390–391:176–83. <https://doi.org/10.1016/j.wear.2017.07.023>.
- [24] Schubert WD, Neumeister H, Kinger G, Lux B. Hardness to toughness relationship of fine-grained WC-Co hardmetals. *Int J Refract Met Hard Mater* 1998;16:133–42. [https://doi.org/10.1016/S0263-4368\(98\)00028-6](https://doi.org/10.1016/S0263-4368(98)00028-6).
- [25] Canovic S, Ljungberg B, Halvarsson M. CVD TiC/alumina multilayer coatings grown on sapphire single crystals. *Micron* 2011;42:808–18. <https://doi.org/10.1016/j.micron.2011.05.003>.
- [26] Canovic S, Ljungberg B, Björmander C, Halvarsson M. CVD TiC/alumina and TiN/alumina multilayer coatings grown on sapphire single crystals. *Int J Refract Met Hard Mater* 2010;28:163–73. <https://doi.org/10.1016/j.ijrmhm.2009.08.001>.
- [27] Santhanam AT, Quinto DT, Grab GP. Comparison of the steel-milling performance of carbide inserts with MTCVD and PVD TiCN coatings. *Int J Refract Met Hard Mater* 1996;14:31–40. [https://doi.org/10.1016/0263-4368\(96\)83415-9](https://doi.org/10.1016/0263-4368(96)83415-9).
- [28] Karlsson L, Hultman L, Johansson MP, Sundgren J-E, Ljungcrantz H. Growth, microstructure, and mechanical properties of arc evaporated TiCxN1–x (0 ≤ x ≤ 1) films. *Surf Coatings Technol* 2000;126:1–14. [https://doi.org/10.1016/S0257-8972\(00\)00518-1](https://doi.org/10.1016/S0257-8972(00)00518-1).